Riminucci, A., & Schwarzacher, W. (2017). Coexistence of superconductivity and superparamagnetism in Pb-Co electrodeposited nanowires. *Applied Physics A: Materials Science and Processing*, *123*, [161]. https://doi.org/10.1007/s00339-017-0782-z

Coexistence of superconductivity and superparamagnetism in Pb-Co electrodeposited nanowires

Alberto Riminucci[1,2], Walther Schwarzacher[2]

[1] CNR-ISMN, Via Gobetti 101, 40129 Bologna, Italy

[2] H.H.Wills Physics Laboratory, Tyndall Avenue, BS8 1TL, Bristol, UK

Abstract

Pb-Co nanowires were electrodeposited in 100 nm nominal pore diameter polycarbonate membranes. Above the T_C of Pb we modelled the behaviour of the wires with a Langevin function, obtaining a Co volume of $(1.06\pm0.01)\times10^{-7}$ cm^3 divided into clusters of ≈10 atoms in size. The magnetic response of the wires in the 3 K to 10 K interval, which comprises T_C, was modelled by adding spherical superconducting Pb grains to the Co clusters; the Pb grains were found to be (87±6) nm in diameter. The Co clusters were not interacting and were not magnetically screened by the superconducting Pb.

Introduction

The interplay between ferromagnetism and superconductivity has received great attention in recent years, both for its fundamental interest [1]–[10] and potential applications in superconducting electronics and quantum computation[11], [12]. Ferromagnetic grains can be embedded in a superconducting matrix [13]–[15], with consequences for the magnetic and microstructural properties of the system. The latter are of special interest, since superconducting properties are strongly affected by microstructure: if a system is granular, the superconductivity can be either intragrain or intergrain [16]. In the former case the grains superconduct separately whereas in the latter the superconductor behaves as a whole, with the grains being linked by Josephson junctions [17], [18]. A small magnetic field (<20 Oe) can destroy the phase coherence between grains and make the superconductor effectively behave as an intragrain one[19]. The incorporation of ferromagnetic impurities between the grains can lead to further interesting effects, ranging from a decrease of the critical temperature

T_C[6], [20] of superconductivity due to the proximity effect[7], [8], to superparamagnetism. The latter refers to the magnetic properties of single-domain clusters of a ferromagnetic metal [21]. At sufficiently low temperatures the magnetic moment of each cluster is pinned in a particular direction by anisotropy. The blocking temperature T_B can then be defined as the temperature at which there is a transition to the superparamagnetic state, in which the thermal energy is sufficient to overcome the anisotropy energy and the direction of the magnetic moment of each grain is free to rotate.

Electrodeposition can be used to fabricate a diverse range of structures such as multilayers[22], [23] and nanowires[24]–[28]; it lends itself naturally to the fabrication of binary granular systems[29] because different metal ions can be deposited simultaneously from the same solution and because the microstructure can be controlled by the growth parameters.

In this work Pb-Co wires were grown in commercially available polycarbonate nanoporous membranes by electrodeposition. The wires were free standing so that interaction with the substrate could be neglected. By assuming that the Pb was made of identical spherical grains, we were able to model their magnetic response. The calculated size of the superconducting grains in Pb-Co wires was found to be similar to that for pure Pb wires. Furthermore, it was possible to calculate the size of the superparamagnetic Co clusters. We found that no magnetic interaction occurred among them and that their magnetic field was not shielded by the superconducting Pb; no evidence of the proximity effect was detected.

EXPERIMENTAL

The Pb-Co nanowires were grown from a 0.5 M $Co(H_2NSO_3)_2$, 0.5 M $Pb(H_2NSO_3)_2$, pH= 4.3 aqueous solution in commercially available polycarbonate membranes with a 100 nm nominal pore diameter, at 27˚C. A 200 nm thick film of Au was evaporated onto one side of the polycarbonate membrane to act as a working electrode (WE). Care was taken to make sure that this film was continuous.

The growth was carried out in a standard electrochemical cell. We used a saturated calomel reference electrode (RE) and a platinum plate as the counter electrode (CE). Growth was carried out

potentiostatically at -0.9 V. The distance between WE, CE and RE was kept constant between each deposition run.

After growth, some of the nanowires were freed from the membranes by dissolving the latter in chloroform, and were studied using a Philips 430 TEM with 250 kV accelerating voltage. For the magnetic characterization, we used a Quantum Design magnetic property measurement system (MPMS) superconducting quantum interference device (SQUID) magnetometer. Samples for SQUID characterization were prepared by cutting an area of 3×4 mm^2 from the membrane. Excess Pb and Co, deposited after the pores had been filled, and the Au substrate were removed by gentle scraping with cotton wool soaked in ethanol. In order to eliminate any possible trapped magnetic flux prior to measurement with the SQUID, the samples were demagnetized by bringing them above T_C in zero applied magnetic field.

RESULTS AND DISCUSSION

The wires were thick enough to be mostly opaque to the TEM electron beam, as shown in Figure 1. They were cigar-shaped, due to the shape of the pores in which they were deposited. Typically, the minimum diameter along a wire was 130 nm and the maximum was 200 nm. The image quality was insufficient to discriminate Co grains from Pb ones. Pb and Co are reported to be immiscible and Co is expected to be present in the Pb matrix in its εCo phase (disordered hcp) [30]. When Pb-Co granular films were grown by e-beam coevaporation in UHV by Luby et al.[31], no alloying was detected.

Measurements of the magnetic moment of arrays of wires were made both at a constant applied field H_a by sweeping the temperature and at constant temperature by sweeping the field. The field was applied perpendicular to the wires' axis.

Above the blocking temperature T_B a superparamagnetic system is expected to follow the Langevin law, with the magnetic moment given by[32]:

$$m = V_M n \mu \left[coth\left(\frac{\mu H_a}{k_B T}\right) - \frac{k_B T}{\mu H} \right] \quad (1)$$

where V_M is the volume of the superparamagnetic fraction, n is the number of nanoparticles per unit volume, μ is the magnetic moment of a grain, k_B is Boltzmann's constant, H_a is the applied magnetic field and T is the absolute temperature; $V_M \cdot n$ is the total number of superparamagnetic particles. Equation (1) shows that scaling of the magnetization curve with H_a/k_BT is a strong indication of superparamagnetism.

Above T_C, that is at a temperature greater than 7.18 K, the screening effect due to the superconducting Pb matrix must vanish almost completely (a faint screening is still present due to the weak diamagnetism of Pb, which has a volume susceptibility of -1.259×10^{-6} emu/cm^3 above T_C). In order to confirm the superparamagnetic behaviour of the Co grains above T_C, we performed *M-H* measurements by sweeping the field at a fixed temperature. The graph in Figure 2 shows the data measured at 10 K. Pb was in its normal state at this temperature and its contribution to the magnetization of the sample could be neglected.

By fitting the curve in Figure 2 with equation (1), we obtained the following values for the Langevin function parameters: $\mu = (17.8\pm0.1)\mu_B$ and $V_M \cdot n = (9.28\pm0.04)\times10^{14}$, which correspond to a total Co volume of $(1.06\pm0.01)\times10^{-7}$ cm^3. Since the magnetization of Co is 1.71 μ_B per atom[33], this value for μ amounts to ~10 atoms per cluster, if we neglect surface effects.

Below T_C, both the diamagnetism due to superconducting Pb and the superparamagnetism of Co can be present at the same time. Figure 3a) shows the magnetic moment as a function of temperature at several constant applied magnetic fields. These curves may be understood as the superposition of a superconducting and a superparamagnetic signal.

To fit the data in Figure 3a), the following equations for the measured magnetic moment m were used:

$$\begin{cases} m = -\frac{3}{8\pi} V_S H_a \left[1 - \frac{3\lambda_L(T)}{a}\coth\left(\frac{a}{\lambda_L(T)}\right) + \frac{3\lambda_L(T)^2}{a^2}\right] + V_M\, n\, \mu \left[coth\left(\frac{\mu H_a}{K_B T}\right) - \frac{k_B T}{\mu H}\right] if\ T < T_C & (2) \\ m = V_M\, n\, \mu \left[coth\left(\frac{\mu H_a}{k_B T}\right) - \frac{k_B T}{\mu H_a}\right] if\ T \geq T_C & (3) \end{cases}$$

where V_S is the volume of the superconducting fraction of the sample, H_a is the applied magnetic field, $\lambda_L(T) = \lambda_L(0)/\sqrt{1-(T/T_C)^4}$, $\lambda_L(0) = 40$ nm is the penetration depth of Pb, and a is the radius of the spherical superconducting grains. The first term of the sum in equation (2) represents the magnetic moment of the superconducting fraction[34] while the second term represents the superparamagnetic fraction of the sample. Above T_C only the superparamagnetic component is present, as indicated by equation (3).

To fit the data above T_C in Figure 3a), we used the value for μ that was obtained from the fit to the data in Figure 2. We obtained $V_M\, n = (14\pm1)\times10^{14}$, which was in fair agreement with the same parameter obtained from the data in Figure 2. These parameters, together with a superconducting volume V_S of $(7\pm1)\times10^{-7}$ cm^3[35], were used to fit the data below T_C in Figure 3a) with equation (2). We obtained a superconducting grain diameter of $2a = (87\pm6)$ nm, which was similar to that of pure Pb nanowires grown with the same technique[35].

The values for V_M·n and μ obtained above, together with a $V_S=7\times10^{-7}$ cm^3, correspond to a Co volume concentration of $C_{Co}= 15$ v\v%. These figure confirms that the volume concentration is well below the percolation limit (29% volume fraction [36]).

When the superparamagnetic component was subtracted from the data in Figure 3a), the data in Figure 3b) were obtained. In order to do this, we used the same parameters for the superparamagnetic component for all applied magnetic fields, to demonstrate that they capture the underlying physical quantities. The resulting data are similar to those one would expect from a sample of pure Pb. Below T_C, the magnetic moment as function of the magnetic field can be understood by considering that there are two limiting magnetic field values that cause a superconductor to have a small magnetic moment: 0 Oe and very high (1200 Oe in this case) applied magnetic field; the maximum magnetic moment is reached at intermediate values of H_a (at 200 Oe in our case). Departures from this trend in Figure 3b) are due to noise. The proximity effect was not detected in our measurements since there

were no measurable changes in the T_C of Pb; this could be due to oxidation of the intergrain boundaries.

At high enough fields, superconductivity in Pb was disrupted, since the critical field of Pb is H_C(3 K)≈ 670 Oe[37]. Therefore, at higher fields, magnetization curves measured at temperatures above and below T_C can be compared directly. Figure 4 shows two *M-H* curves measured at 3 K and 10 K. Since the Langevin function has $\mu H_a/(k_B T)$ as an argument, plotting the magnetic moment as a function of $H_a/k_B T$ should give two identical curves for a superparamagnetic system. This is exactly what happens in Figure 4, apart from a small superconducting contribution below H_C. This demonstrates that the sample is superparamagnetic. The fact that the sample is superparamagnetic implies that the Co grains do not interact with each other so that they must be distributed fairly homogeneously along the wire. More importantly, the absence of a change in amplitude of the curves means that there is no significant screening of the Co magnetic signal due to the Meissner effect below T_C and confirms the validity of the procedure. The lack of screening might be due to several reasons. The penetration depth of the applied magnetic field in Pb (40 nm) was of the same order of magnitude as the radius of the wires (100 nm at most) so that the total screening effect will be significantly less than if the Co grains were surrounded by bulk Pb. Also, the Co could be distributed preferentially at the surface of the wires. The inset in Figure 4 shows the data taken at 3 K after the superparamagnetic contribution was subtracted. The behaviour is similar to that of pure Pb nanowires[35]. Some hysteresis was present, and can be attributed either to magnetic flux trapped into the superconductor or to supercooling of the intermediate state[38], [39].

Conclusions

We have electrodeposited Pb-Co granular nanowires and proposed a model for the behaviour of their magnetic moment in the presence of an applied magnetic field. We were able to model the superparamagnetic response of the sample by considering Co grains ~10 atoms in size, confirming that Co was not dispersed into the Pb but that it formed clusters. We further estimated the Pb grain

size from the magnetic response in the superconducting state, obtaining a value of (87±6) nm, with no evidence of the proximity effect. We estimated that a Co concentration of 15 v\v% was present. Finally, we found that the Co clusters were non interacting and were not magnetically screened by the superconducting Pb. The fact that both the magnetic properties of the Co and the superconducting ones of Pb were well preserved in our samples, bodes well for the application of this technique to the fabrication of devices based on superconducting/ferromagnetic systems, which have possible applications in quantum computing.

[1] I. F. Lyuksyutov and V. L. Pokrovsky, “Ferromagnet–superconductor hybrids,” *Adv. Phys.*, vol. 54, no. 1, pp. 67–136, 2005.

[2] S. M. Frolov, D. J. Van Harlingen, V. A. Oboznov, V. V. Bolginov, and V. V. Ryazanov, “Measurement of the current-phase relation of superconductor/ferromagnet/ superconductor ?? Josephson junctions,” *Phys. Rev. B - Condens. Matter Mater. Phys.*, vol. 70, no. 14, pp. 1–5, 2004.

[3] V. V. Ryazanov, V. A. Oboznov, A. Y. Rusanov, A. V. Veretennikov, A. A. Golubov, and J. Aarts, “Coupling of two superconductors through a ferromagnet: Evidence for a π junction,” *Phys. Rev. Lett.*, vol. 86, no. 11, pp. 2427–2430, 2001.

[4] C. Bell, R. Loloee, G. Burnell, and M. G. Blamire, “Characteristics of strong ferromagnetic Josephson junctions with epitaxial barriers,” *Phys. Rev. B - Condens. Matter Mater. Phys.*, vol. 71, no. 18, pp. 2–5, 2005.

[5] M. Lange, M. J. Van Bael, and V. V Moshchalkov, “Vortex matter in superconductor/ferromagnet hybrids,” *J. Low Temp. Phys.*, vol. 139, no. 1, pp. 195–206, 2005.

[6] K. Neuróhr, J. Dégi, L. Pogány, I. Bakonyi, D. Ungvári, K. Vad, J. Hakl, Á. Révész, and L. Péter, “Composition, morphology and electrical transport properties of Co-Pb electrodeposits,” *J. Alloys Compd.*, vol. 545, pp. 111–121, 2012.

[7] A. I. Buzdin, “Proximity effects in superconductor-ferromagnet heterostructures,” *Rev. Mod. Phys.*, vol. 77, no. 3, pp. 935–976, 2005.

[8] J. Xia, V. Shelukhin, M. Karpovski, A. Kapitulnik, and A. Palevski, “Inverse proximity effect in superconductor-ferromagnet bilayer structures,” *Phys. Rev. Lett.*, vol. 102, no. 8, pp. 1–4, 2009.

[9] M. M. Doria, A. R. de C. Romaguera, M. V Milošević, and F. M. Peeters, “Threefold onset of vortex loops in superconductors with a magnetic core,” *Europhys. Lett.*, vol. 79, no. 4, p.

47006, 2007.

[10] G. C. Ménard, S. Guissart, C. Brun, M. Trif, F. Debontridder, R. T. Leriche, D. Demaille, D. Roditchev, P. Simon, and T. Cren, "Two-dimensional topological superconductivity in Pb/Co/Si(111)," *Condens. Matter - Supercond.*, no. 111, pp. 1–12, 2016.

[11] A. Ruotolo, G. P. Pepe, C. Bell, C. W. Leung, and M. G. Blamire, "Modulation of the dc Josephson current in pseudo-spin-valve Josephson multilayers," *Supercond. Sci. Technol.*, vol. 18, no. 6, pp. 921–926, 2005.

[12] J. J. A. Baselmans, B. J. Van Wees, and T. M. Klapwijk, "Controllable π SQUID," *Appl. Phys. Lett.*, vol. 79, no. 18, pp. 2940–2942, 2001.

[13] S. P. Kruchinin, Y. I. Dzhezherya, and J. F. Annett, "Interactions of nanoscale ferromagnetic granules in a London superconductor," *Supercond. Sci. Technol.*, vol. 19, pp. 381–384, 2006.

[14] Y. T. Xing, H. Micklitz, T. G. Rappoport, M. V. Milošević, I. G. Solórzano-Naranjo, and E. Baggio-Saitovitch, "Spontaneous vortex phases in superconductor-ferromagnet Pb-Co nanocomposite films," *Phys. Rev. B - Condens. Matter Mater. Phys.*, vol. 78, no. 22, pp. 1–5, 2008.

[15] A. Palau, H. Parvaneh, N. A. Stelmashenko, H. Wang, J. L. MacManus-Driscoll, and M. G. Blamire, "Hysteretic vortex pinning in superconductor-ferromagnet nanocomposites," *Phys. Rev. Lett.*, vol. 98, no. 11, pp. 2–5, 2007.

[16] H. F. Hebard, "Experimental results on the Nature of the Superconducting-Insulating Transition in Two Dimensions," in *STRONGLY CORRELATED ELECTRONIC MATERIALS - THE LOS ALAMOS SYMPOSIUM*, K. S. Bedell, Z. Q. Wang, D. E. Meltzer, A. V. Balatsky, and E. Abrahams, Eds. ADDISON-WESLEY, 1994, pp. 251–278.

[17] Y. M. Chiang, D. A. Rudman, D. K. Leung, J. A. . Ikeda, A. Roshko, and B. D. Fabes, "EFFECTS OF GRAIN SIZE AND GRAIN-BOUNDARY SEGREGATION ON SUPERCONDUCTING PROPERTIES OF DENSE POLYCRYSTALLINE La1.85Sr0.15CuO4," *Phys. C-SUPERCONDUCTIVITY ITS Appl.*, vol. 152, pp. 77–90, 1988.

[18] D. Sharma, R. Kumar, H. Kishan, and V. P. S. Awana, “Influence of Grain Size on the Superconductivity of La1.85Sr0.15CuO4,” *J. Supercond. Nov. Magn.*, vol. 24, no. 1–2, pp. 205–209, 2011.

[19] S. Sarangi, S. P. Chockalingam, and S. V. Bhat, “Frequent Josephson junction decoupling is the main origin of ac losses in the superconducting state,” *J. Appl. Phys.*, vol. 98, no. 7, pp. 0–5, 2005.

[20] K. Schwidtal, “Supraleitung aufgedampfter Bleischichten mit Zusatz von Gadolinium,” *Zeitschrift fur Phys.*, vol. 158, no. 5, pp. 563–571, 1960.

[21] B. D. Cullity and C. D. Graham, *Introduction to Magnetic Materials*, Second. Wiley-IEEE Press, 2008.

[22] C. A. Ross, “Electrodeposited Multilayer Thin Films,” *Annu. Rev. Mater. Sci.*, vol. 24, no. 1, pp. 159–188, 1994.

[23] I. Bakonyi and L. Péter, “Electrodeposited multilayer films with giant magnetoresistance (GMR): Progress and problems,” *Prog. Mater. Sci.*, vol. 55, no. 3, pp. 107–245, 2010.

[24] Yi G, Schwarzacher W, “Single crystal superconductor nanowires by electrodeposition,” *Appl. Phys. Lett.*, vol. 74, no. 12, pp. 1746–1748, 1999.

[25] D. Y. Vodolazov, F. M. Peeters, L. Piraux, S. Mátéfi-Tempfli, and S. Michotte, “Current-Voltage Characteristics of Quasi-One-Dimensional Superconductors: An S-Shaped Curve in the Constant Voltage Regime,” *Phys. Rev. Lett.*, vol. 91, no. 15, p. 157001(1-4), 2003.

[26] Michotte S, Matefi-Tempfli S and Piraux L, “Current-voltage characteristics of Pb and Sn granular superconducting nanowires,” *Appl. Phys. Lett.*, vol. 82, no. 23, pp. 4119–4121, 2003.

[27] S.Dubois, A.Michel, J.P.Eymery, J.L.Duvail and L.Piraux, “Fabrication and properties of arrays of superconducting nanowires,” *J. Mater. Res.*, vol. 14, no. 3, pp. 665–671, 1999.

[28] M. A. Engbarth, S. J. Bending, and M. V. Milošević, “Geometry-driven vortex states in type-I superconducting Pb nanowires,” *Phys. Rev. B - Condens. Matter Mater. Phys.*, vol. 83, no.

22, pp. 1–7, 2011.

[29] W. Schwarzacher, O. I. Kasyutich, P. R. Evans, M. G. Darbyshire, G. Yi, V. M. Fedosyuk, F. Rousseaux, E. Cambril, and D. Decanini, "Metal nanostructures prepared by template electrodeposition," *J. Magn. Magn. Mater.*, vol. 198, pp. 185–190, 1999.

[30] T. B. Massalski, *Binary Alloy Phase Diagrams*. American Society for Metals, Metals Park, Ohio 44073: William W. Scott, Jr., 1986.

[31] S. Luby, E. Majkova, M. Jergel, R. Senderak, E. D'Anna, G. Leggieri, A. Luches, and M. Martino, "Structure and in-depth concentrations in excimer laser irradiated Pb-Co codeposited films," *Thin Solid Films*, vol. 359, no. 2, pp. 141–145, 2000.

[32] IIF-IIR, *Cryogénie. Ses applications en supraconductivité*. IIF-IIR, 1995.

[33] J. M. D. Coey, *Magnetism and Magnetic Materials*. Cambridge: Cambdridge University Press, 2009.

[34] F. London, *Superfluids, volume Volume I: Macroscopic theory of Superconductivity*, Second rev. Dover Publications, Inc., New York, 1960.

[35] A. Riminucci and W. Schwarzacher, "Magnetic signature of granular superconductivity in electrodeposited Pb nanowires," *J. Appl. Phys.*, vol. 115, no. 22, p. 223910, Jun. 2014.

[36] R. Consiglio, D. R. Baker, G. Paul, and H. E. Stanley, "Continuum percolation thresholds for mixtures of spheres of different sizes," *Phys. A Stat. Mech. its Appl.*, vol. 319, pp. 49–55, 2003.

[37] G. Chanin and J. P. Torre, "Critical-field curve of superconducting lead," *Phys. Rev. B*, vol. 5, no. 11, pp. 4357–4364, 1972.

[38] M. Desirant, D. Shoenberg, "The Intermediate State of Superconductors. I. Magnetization of Superconducting Cylinders in Transverse Magnetic Fields," *Proc. R. Soc. Lond. A. Math. Phys. Sci.*, vol. 194, no. 1036, pp. 63–79, 1948.

[39] T. E. Faber, "The Phase Transition in Superconductors. I. Nucleation," *Proc. R. Soc. Lond. A. Math. Phys. Sci.*, vol. 214, no. 1118, pp. 392–412, 1952.

[40] M. Tinkham and P. G. De Gennes, “Mangetic behavior of very small superconducting particles,” *Physics (College. Park. Md).*, vol. 1, no. 2, pp. 107–126, 1964.

Captions

Figure 1: Transmission electron microscope (TEM) image of the nanowires. The wires were cigar-shaped, reflecting the shape of the pores in which they grew. On average the minimum diameter along a wire was 130 nm and the maximum was 200 nm.

Figure 2: *M-H* curve for the Pb-Co wires measured at 10 K. At this temperature the Pb is not superconducting and only the superparamagnetic signal is present.

Figure 3: a) Temperature sweeps at different magnetic fields. The signal consists of two superimposed components: a superparamagnetic one and a superconducting one. Pb becomes superconducting below 7.18 K at 0 Oe applied field and its superconducting transition is responsible for the kinks observed in the curves at that temperature. The red lines represent the fits carried out with equation (2) below 7.18 K and with equation (3) above it. b) Data from a) after subtraction of the superparamagnetic signal, calculated with the fitting parameters for the data in Figure 2. The superconducting transition at 7.18 K becomes apparent. The superconducting transition is not sharp because the grains forming the wire have a finite size distribution. At a given field, smaller grains have a higher T_C [40]. The magnetic moment of the superconductor has maximum magnitude at 200 Oe, and decreases for lower and higher fields.

Figure 4: *M-H* curves for Pb-Co wires measured at 3 K and 10 K. The superposition of the two curves (apart from the deviation caused by superconductivity below $H_C(3\ K) \approx 670$ Oe, that is for $|H/k_BT| < 1.62\times10^{18}$ Oe/erg) is a signature of superparamagnetism. Also, the superposition shows that the superparamagnetic signal is not screened by the superconducting Pb. The inset shows the data at 3 K after the superparamagnetic contribution was subtracted; the noise is due to the large contribution to the magnetic signal coming from superparamagnetic phase. The behaviour is similar to that of pure Pb nanowires[35], including the hysteresis.

Figure 1

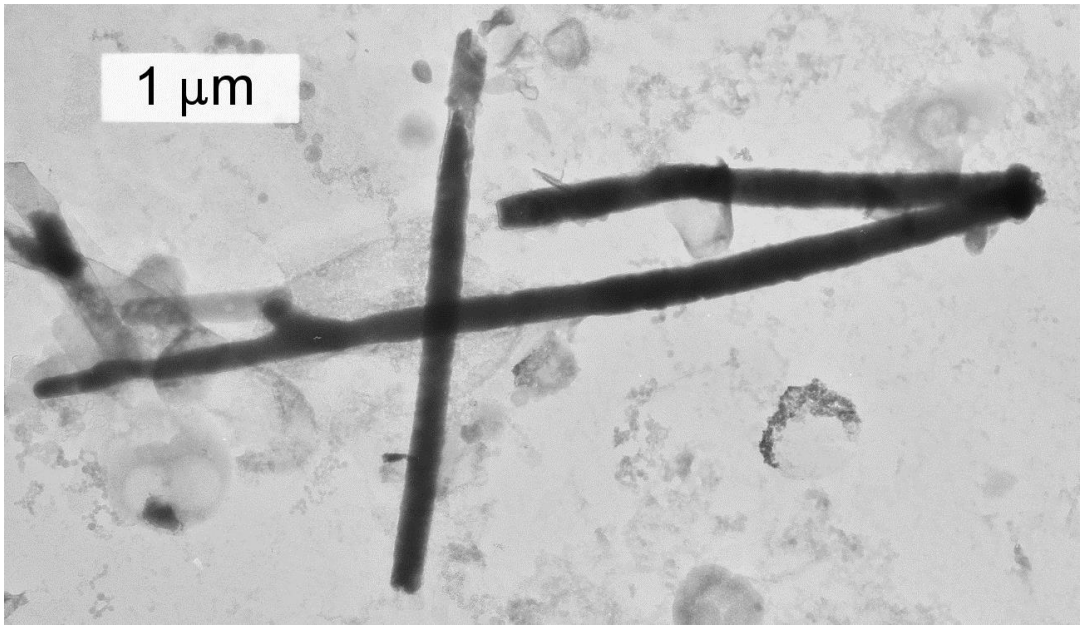

Figure 2

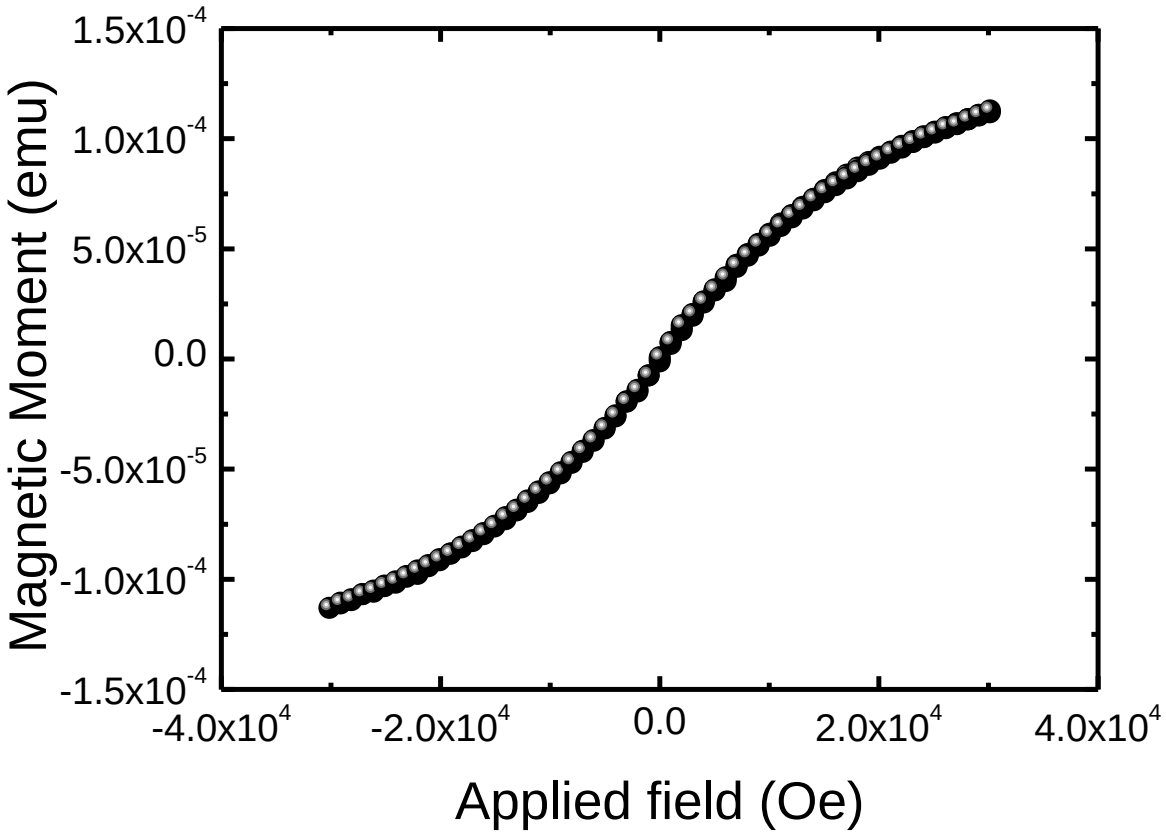
Magnetic Moment (emu)
1.5x10-4
1.0x10-4
5.0x10-5
0.0
-5.0x10-5
-1.0x10-4
-1.5x10-4
-4.0x10^4
-2.0x10^4
0.0
2.0x10^4
4.0x10^4
Applied field (Oe)

Figure 3

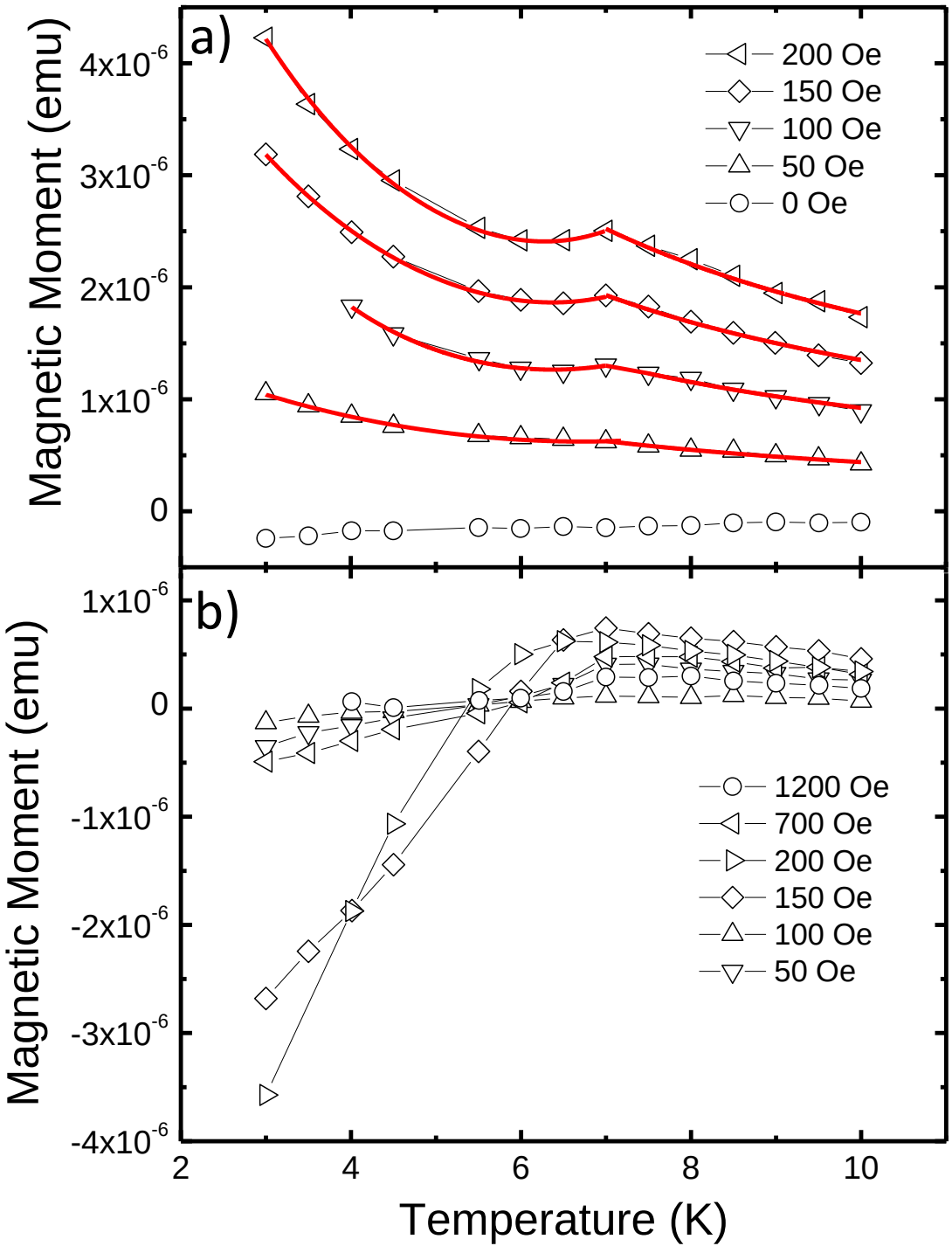
a)
200 Oe
150 Oe
100 Oe
50 Oe
0 Oe
Magnetic Moment (emu)
4x10-6
3x10-6
2x10-6
1x10-6
0
b)
1200 Oe
700 Oe
200 Oe
150 Oe
100 Oe
50 Oe
Magnetic Moment (emu)
1x10-6
0
-1x10-6
-2x10-6
-3x10-6
-4x10-6
2
4
6
8
10
Temperature (K)

Figure 4

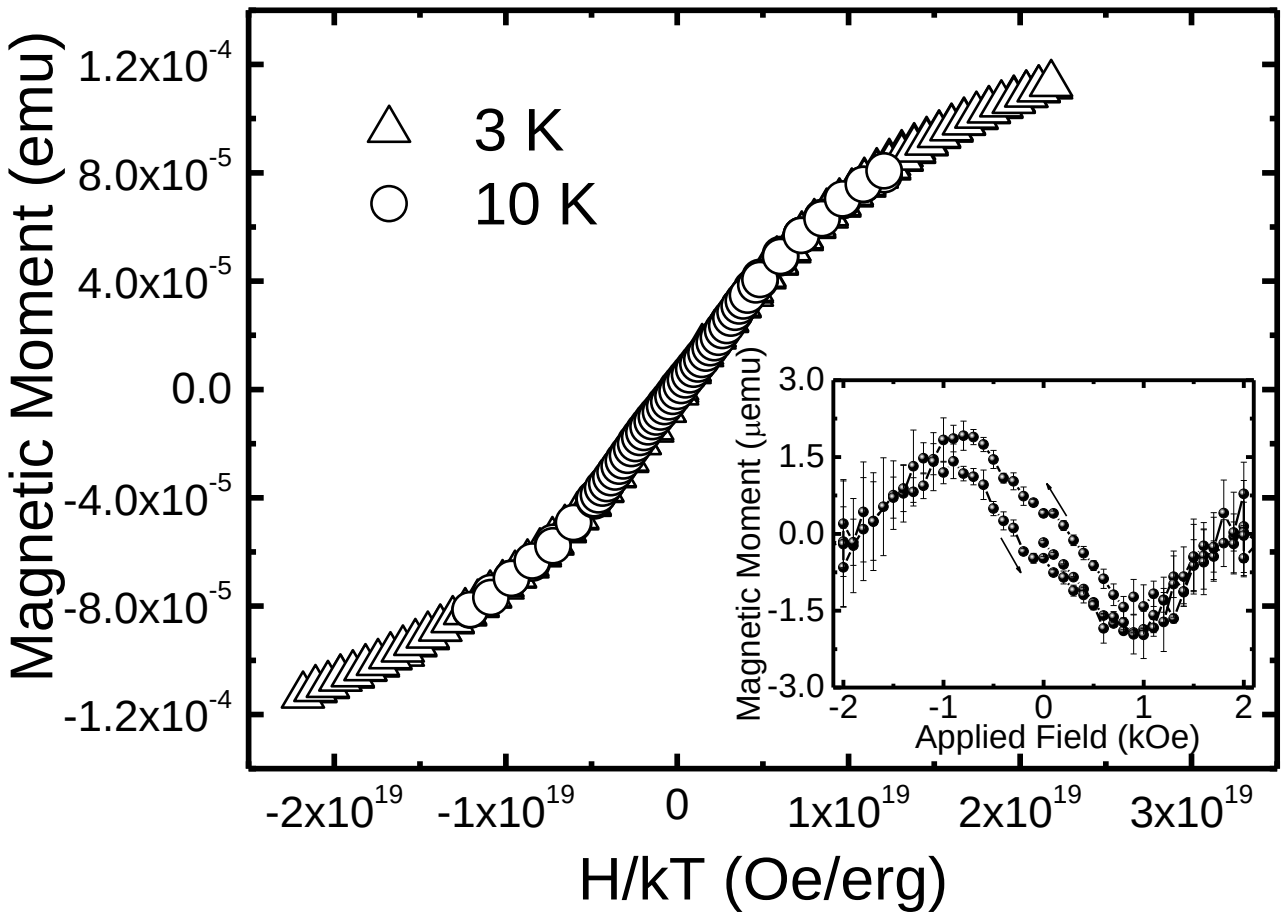
Magnetic Moment (emu)
1.2x10-4
8.0x10-5
4.0x10-5
0.0
-4.0x10-5
-8.0x10-5
-1.2x10-4
3 K
10 K
-2x1019
-1x1019
0
1x1019
2x1019
3x1019
H/kT (Oe/erg)
Magnetic Moment (μemu)
3.0
1.5
0.0
-1.5
-3.0
-2
-1
0
1
2
Applied Field (kOe)